

# STRUCTURAL STUDIES OF MATERIALS FOR HYDROGEN STORAGE

***Final report (preliminary<sup>a</sup>) - High Resolution SR-PXD measurement: 01-01-745  
Beamline BM01B***

## **Initial comment**

The Physics Department at Institute for Energy Technology has a strong activity on hydrogen storage materials, involving many national and international collaborators. The strong position of the group is to a high degree owing to the good access to neutrons for powder neutron diffraction (PND) using the diffractometer PUS at the Institute's research reactor JEEP II.

Synchrotron power X-ray diffraction (SR-PXD) is an invaluable supplement to PND due to the superior speed and resolution. The data acquisition times are typically 3 orders of magnitude shorter using the MAR345 image plate at BM01A compared to PUS. This allows in-situ investigations of chemical reactions that we cannot possibly follow with PND. The very high resolution offered at BM01B allows indexing and space group determination from complex structures where the problem with peak overlapping makes the task unmanageable with PND- or laboratory PXD data.

Thus, the predictable, long-term access to the beam lines at SNBL through the long-term projects 01-01-745 and 01-02-772, has been an invaluable supplement to our neutron diffraction facilities and the rest of our experimental activity.

## **The crystal structures of $\text{LiMg}(\text{AlD}_4)_3$ and $\text{LiMgAlD}_6$**

'Alانات' ( $\text{AlH}_4^-$  or  $\text{AlH}_6^{3-}$  based complex hydrides) have been extensively investigated since the discovery of reversible hydrogen desorption from Ti-enhanced  $\text{NaAlH}_4$ .

The mixed alانات  $\text{LiMg}(\text{AlH}_4)_3$  and its thermal decomposition product  $\text{LiMgAlH}_6$  have been known since 1970, but their crystal structures have remained unknown.

Deuterated  $\text{LiMg}(\text{AlD}_4)_3$  was synthesised by ball milling  $\text{LiAlD}_4$  and  $\text{MgCl}_2$ , yielding a mixture of poorly crystalline  $\text{LiMg}(\text{AlD}_4)_3$  and  $\text{LiCl}$ . Purer (~10wt%  $\text{LiCl}$ ), well-crystalline  $\text{LiMg}(\text{AlD}_4)_3$  was obtained by recrystallization in diethyl ether.

High-resolution SR-PXD data were collected at BM01B and used for indexing and space group determination ( $a = 8.37113(16) \text{ \AA}$ ,  $b = 8.73910(17) \text{ \AA}$ ,  $c = 14.3012(3) \text{ \AA}$  and  $\beta = 124.8308(8)^\circ$ , space group  $P2_1/c$ ). The data were used in combination with high-resolution PND data from the PUS diffractometer at the JEEP II reactor (Kjeller, Norway) for ab-initio structure determination using the global optimization approach. The structure model was refined by according to the Rietveld method (Figure 1).

---

<sup>a</sup> One experimental session (15 shifts) for the long-term project 01-01-745 remains and will be performed in 5-10 March 2009.

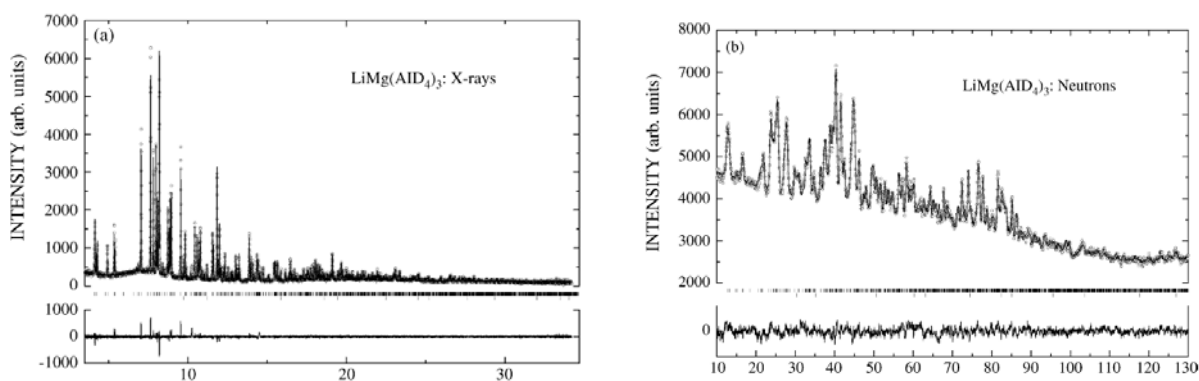


**Figure 1** Rietveld fits of  $\text{LiMg}(\text{AlD}_4)_3$  to a) SR-PXD data and b) PND data. Upper and lower tick marks show Bragg peaks from  $\text{LiMg}(\text{AlD}_4)_3$  and  $\text{LiCl}$ , respectively.

Both Li and Mg were found to be octahedrally coordinated by D atoms from six different  $\text{AlD}_4$  tetrahedra. Thus, the crystal structure of  $\text{LiMg}(\text{AlD}_4)_3$  can be regarded as a corner-sharing network of  $\text{LiD}_6$  and  $\text{MgD}_6$  octahedra and  $\text{AlD}_4$  tetrahedra. Moreover, the  $\text{AlD}_4$  form a distorted hexagonal close-packed lattice, which thus have Li or Mg in 2/3 of the octahedral interstices. execute

A mixture of  $\text{LiMgAlD}_6$  and Al was prepared by thermal decomposition of  $\text{LiMg}(\text{AlD}_4)_3$ . The product was measured by high-resolution SR-PXD (BM01B) and PND (PUS, JEEP II). A structure model was already predicted from DFT calculations (unpublished). Rietveld refinement was performed against the SR-PXD and PND simultaneously, and the DFT model was basically confirmed with minor modifications (space group  $P321$   $a = 7.9856(4)$  Å  $c = 4.3789(3)$  Å) (Figure 2)

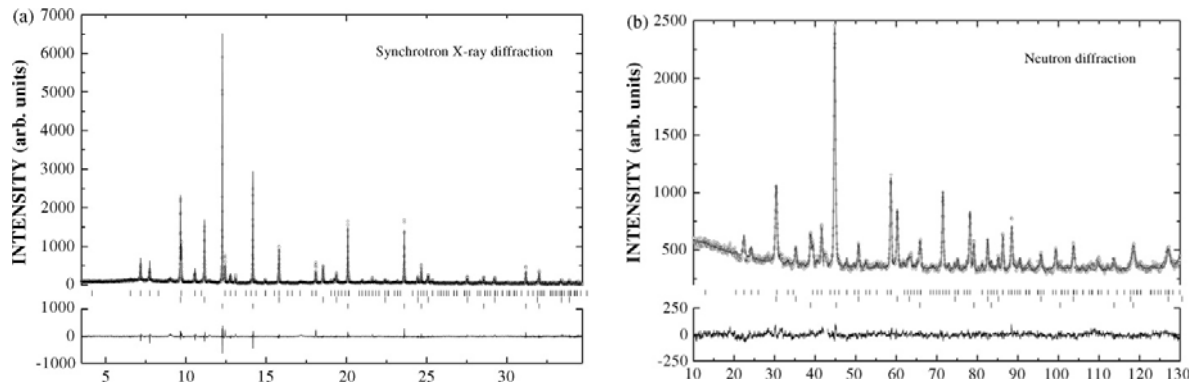


**Figure 2** Rietveld fits of  $\text{LiMgAlD}_6$  to a) SR-PXD data and b) PND data. Upper, middle and lower tick marks show Bragg peaks from  $\text{LiMgAlD}_6$ ,  $\text{LiCl}$  and Al, respectively.

The results are published in two separate papers in Journal of Alloys and Compounds [1, 2].

### Fluorine-substitution in $\text{Na}_3\text{AlD}_6$

Metal-substitution is widely used in intermetallic metal hydrides to alter the properties. Complex hydrides, on the other hand, show very limited possibilities for cation substitution. However, we have found that fluoride anions can substitute hydrogen anions in  $\text{Na}_3\text{AlH}_6$ . The anion-substituted phase was produced by hydrogenating a mixture NaF and Al catalysed with  $\text{TiF}_3$ .

The product was characterized by high-resolution SR-PXD at BM01B and PND with the PUS diffractometer. The data show that that a phase which is isostructural to  $\text{Na}_3\text{AlD}_6$  and  $\text{Na}_3\text{AlF}_6$  was formed. Due to the excellent scattering contrast between D and F with X-rays and the visibility of D for the neutrons, the structure and composition,  $\text{Na}_3\text{AlD}_{1.95}\text{F}_{4.05}$  could

be reliably refined. There is no indication of long-range ordering between the F and D. Quantitative phase analysis showed that the sample contained about 33w% of the anion-substituted alane.

PCT measurement has shown that the anion-substitution has a pronounced destabilizing effect compared to pure  $\text{Na}_3\text{AlD}_6$ .

The results are published in Journal of Physical Chemistry C [3].

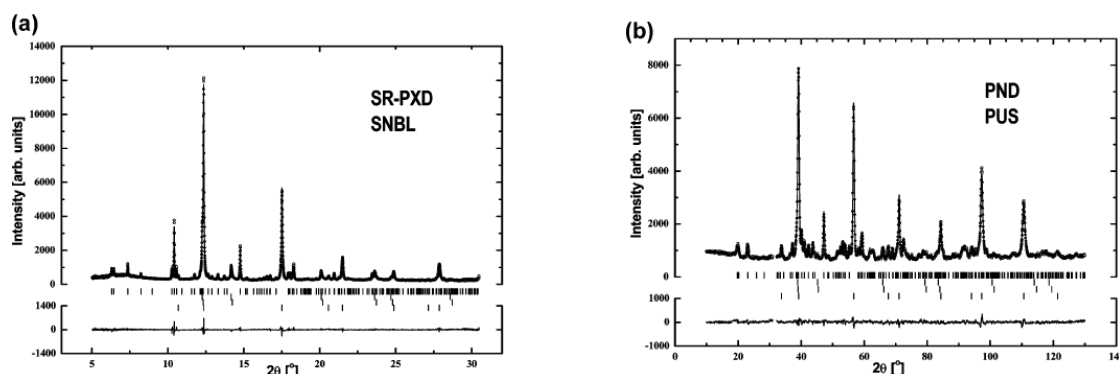


Figure 3 Rietveld fits of to a) SR-PXD data and b) PND data. Tick marks from top to bottom show Bragg peaks from  $\text{Na}_3\text{AlD}_{6-x}\text{F}_x$ , Al,  $\text{Al}_{1-x}\text{Ti}_x$  and NaF.

### **$\text{CaB}_2\text{H}_2$ - an intermediate decomposition product from $\text{Ca}(\text{BH}_4)_2$**

$\text{Ca}(\text{BH}_4)_2$  is considered as an attractive hydrogen storage material due to high gravimetric capacity and expected thermodynamic properties suitable for mobile hydrogen storage applications. However, the decomposition route of this compound is unclear and appears to be highly dependent on the experimental conditions.

In samples partly decomposed in our home laboratory “Temperature Programmed Desorption” (TPD) set-up, we have observed formation of an intermediate phase which is not observed in our recent in-situ SR-PXD measurements [4]. The phase appears during the first decomposition step of  $\text{Ca}(\text{BH}_4)_2$ . A sample which was rich in this intermediate phase, was produced by stopping the TPD right after the first desorption step (370 °C) and quickly cool to room temperature. The sample was measured with high-resolution SR-PXD at BM01B and the data could be indexed according to the orthorhombic unit cell  $a = 12.81 \text{ \AA}$ ,  $b = 4.08 \text{ \AA}$ ,  $c = 3.90 \text{ \AA}$ . The extinction rules pointed to the space groups  $Pnma$  or  $Pbna$ . However, no structure solution succeeded in these space groups. Due to the high number of possible space groups with less systematic absent, a search for isostructural phases with similar unit cell and reasonable stoichiometry was performed in the ICSD database. A model based on the  $\text{HgCl}_2$ -type structure (space group  $Pnma$ ) yielded a superior fit to the experimental data compared to all other evaluated structure types.

Rietveld refinement of the with Ca and B alone (substituted for Hg and Cl, respectively) yielded a satisfactory fit to the SR-PXD data. Two hydrogen positions were located by Difference Fourier Mapping, indicating a total composition  $\text{CaB}_2\text{H}_2$ .

The structure model is shown in Figure 5. It consists of layers Ca atoms which are separated by alternating B layers and layers with infinite  $\text{BH}_2$ -chains. The chains consist of direct -B-H-B-H- links with a terminal H on each boron atom. This is a structural feature which is not reported in any other B-H containing phases and should thus be confirmed with neutron

diffraction. However, due to the strong absorption in natural boron and incoherent scattering from natural hydrogen, a double isotope substituted sample,  $\text{Ca}^{11}\text{B}_2\text{D}_2$  sample must be prepared. This work is in progress.

The results are published in Journal of Materials Chemistry [5].

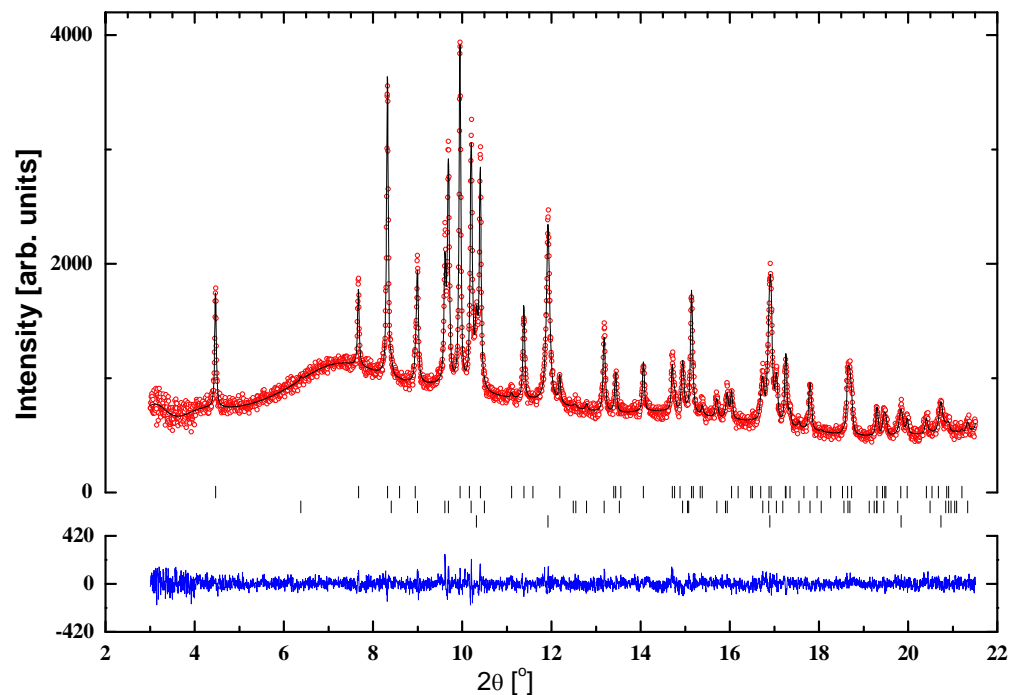


Figure 4 Rietveld fit for the  $\text{CaB}_2$  sublattice of the proposed  $\text{CaB}_2\text{H}_x$ -phase showing observed. The positions of Bragg reflections are shown from  $\text{CaB}_2\text{H}_x$  (upper),  $\text{CaH}_2$  (middle) and  $\text{CaO}$  (lower).

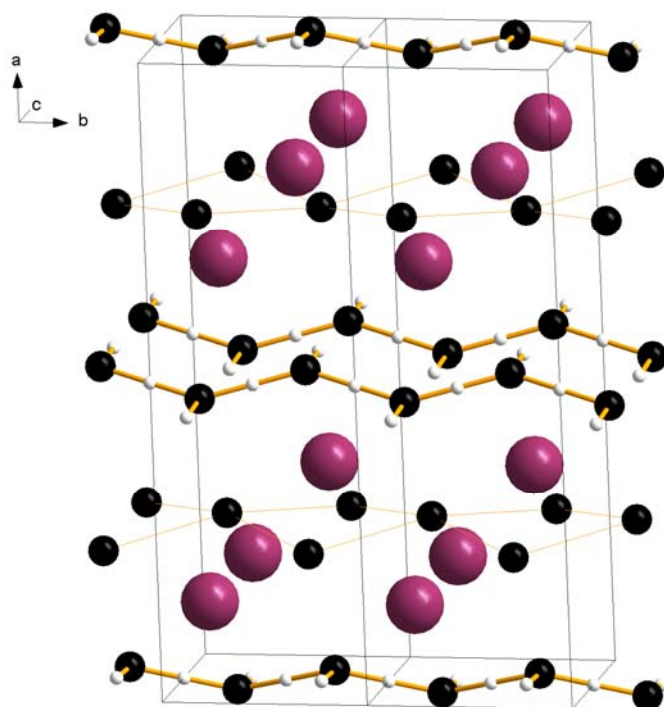


Figure 5 Proposed crystal structure of  $\text{CaB}_2\text{H}_2$ .

### The crystal structure of $\text{LiSc}(\text{BH}_4)_4$

A new mixed borohydrides,  $\text{LiSc}(\text{BH}_4)_3$  was synthesized at Hawaii University. Lab-PXD data revealed a highly crystalline product with no resemblance to any phases in the PDF-4. The data could be indexed according to a cubic unit cell with  $a = 6.08 \text{ \AA}$ . However, the superior resolution at BM01B revealed a slight but significant peak splitting, indicating lower symmetry (see inset in Figure 6). The pattern was successfully indexed with a pseudo-cubic tetragonal unit cell,  $a = 6.076 \text{ \AA}$  and  $c = 12.034 \text{ \AA}$ . The crystal structure was solved and refined in space group  $P-42c$  (Figure 6)

The structure consist of a  $\text{Sc}(\text{BH}_4)_4^-$  complex anions with tetrahedral coordination of 4  $\text{BH}_4$  around Sc. The Li ions where found to be highly disordered and the Li position had to be splitt in two half-occupied positions to get a good agreement with SR-PXD data in the Rietveld refinement (Figure 7). It is suspected that the disorder is dynamic and thus that  $\text{LiSc}(\text{BH}_4)_4$  is a Li-ion conductor.

The results are published in The Journal of Physical Chemistry A [6].

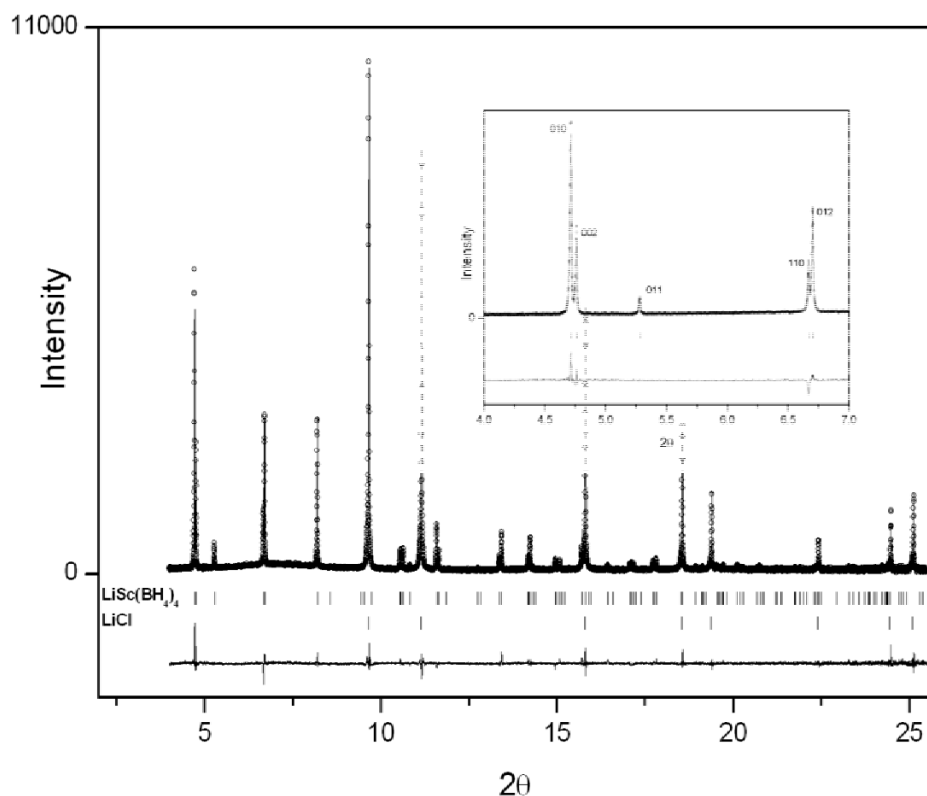
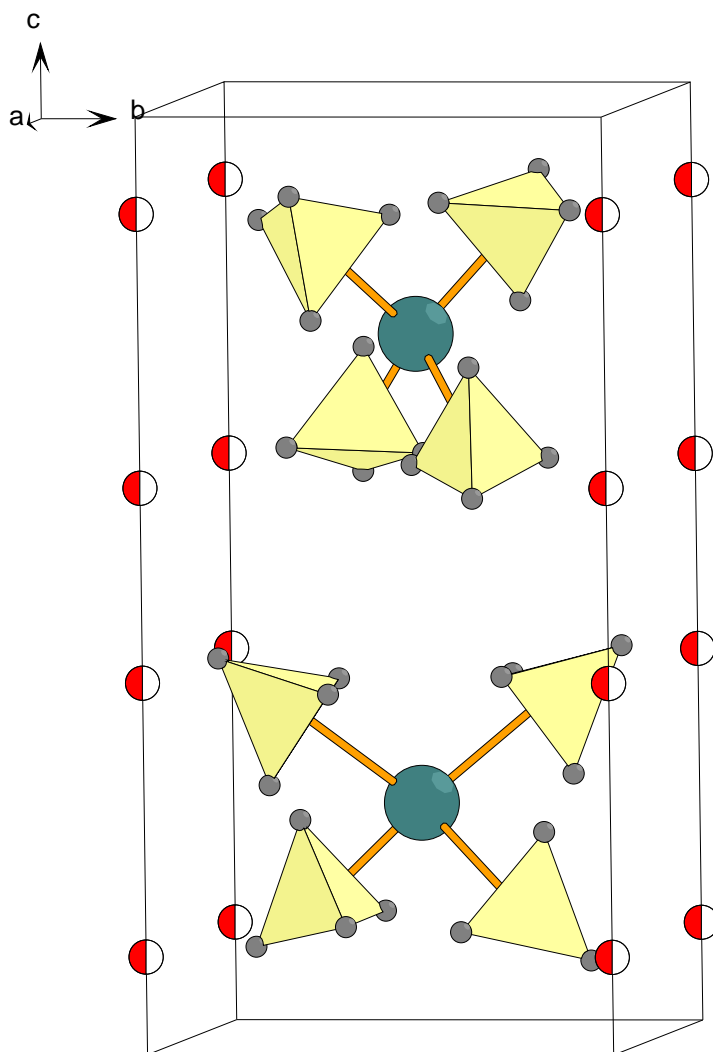


Figure 6 Rietveld fit of  $\text{LiSc}(\text{BH}_4)_4$  to SR-PXD data. The subtle peak splitting due to pseudo-cubic unit cell is shown inset.



**Figure 7 Refined structure of  $\text{LiSc}(\text{BH}_4)_4$ . Large green balls – Sc, tetrahedra –  $\text{BH}_4$ , red and white balls – half-occupied Li sites.**

### **Crystal structure of $\text{Mg}_2(\text{Fe}_{0.5}\text{Co}_{0.5})\text{D}_{5.5}$**

Magnesium hydride,  $\text{MgH}_2$ , has an attractive gravimetric hydrogen content of 7.6 w%H, but is too stable for most hydrogen storage purposes. Magnesium-based transition-metal complex hydrides, e.g.  $\text{Mg}_2\text{NiH}_4$ ,  $\text{Mg}_2\text{FeH}_6$  and  $\text{Mg}_2\text{CoH}_5$ , have more favourable thermodynamics at the expense of lower gravimetric hydrogen content (3.6-5.5 w%H in the given examples). The volumetric hydrogen density is superb.  $\text{Mg}_2\text{FeH}_5$  contains 150  $\text{g}_\text{H}/\text{liter}$ , which is the highest density in known hydrogen storage materials.

A mixed complex hydride,  $\text{Mg}_2(\text{Fe}_{0.5}\text{Co}_{0.5})\text{D}_{5.5}$ , was prepared by ball milling a 1:1 mixture of  $\text{Mg}_2\text{FeD}_6$  and  $\text{Mg}_2\text{CoD}_5$ . A homogeneous cubic face, isostructural to  $\text{Mg}_2\text{FeH}_6$ , was confirmed by SR-PXD at BM01B. No traces of tetragonal  $\text{Mg}_2\text{CoH}_5$  were detected, but small amounts of FeCo solid solution were present.

The crystal structure was refined with the SR-PXD data and PND data from PUS (JEEPII) (Figure 8). The structure is very similar to  $\text{Mg}_2\text{FeD}_6$  and the high-temperature phase of  $\text{Mg}_2\text{CoD}_5$  which constitute fcc packing of  $\text{FeD}_6$  octahedra and  $\text{CoD}_5$  square pyramids (randomly oriented), respectively. Mg is found in all tetrahedral interstices. The transition metals are randomly distributed over the fcc sites in  $\text{Mg}_2(\text{Fe}_{0.5}\text{Co}_{0.5})\text{D}_{5.5}$ . The coordination of the fcc site was refined as a octahedron with  $5/6^{\text{th}}$  of a deuterium atom in each corner. This is

interpreted as a random distribution of  $\text{FeD}_6$  octahedra and  $\text{CoD}_5$  square pyramids since the square pyramid is essentially an octahedron with one missing corner. As in the high-temperature phase of  $\text{Mg}_2\text{CoD}_5$ , there is no long-range correlations in the orientation of the square pyramids.

The results are accepted for publication in Nanotechnology [7].

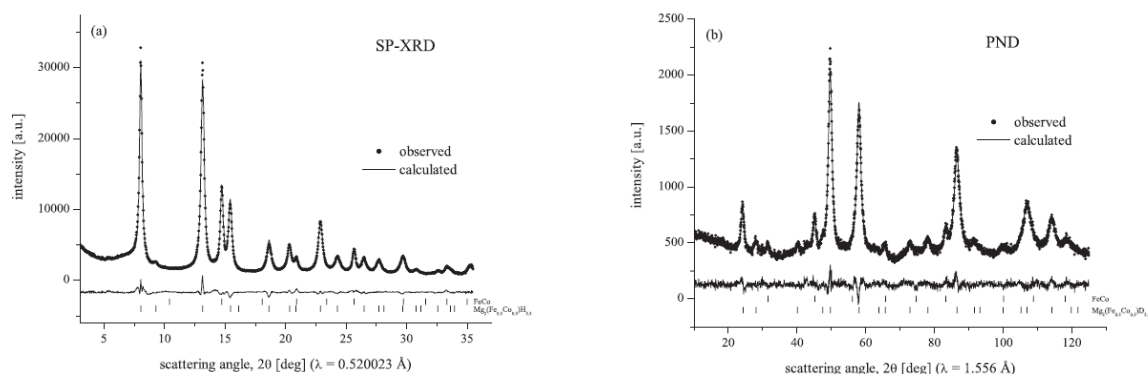


**Figure 8** Rietveld fits of  $\text{Mg}(\text{Fe}_{0.5}\text{Co}_{0.5})\text{D}_{5.5}$  to a) SR-PXD data and b) PND data. Upper and lower tick marks show Bragg peaks from FeCo solid solution and  $\text{Mg}(\text{Fe}_{0.5}\text{Co}_{0.5})\text{D}_{5.5}$ , respectively.

### The crystal structure of $\text{Ca}(\text{AlD}_4)_2$

The existence of  $\text{Ca}(\text{AlH}_4)_2$  has been known for some time, but it has proven difficult to synthesis the solvent-free phase by wet chemical methods. Solvent free  $\text{Ca}(\text{AlD}_4)_2$  was prepared by ball milling  $\text{CaD}_2$  and  $\text{AlD}_3$  in the proper stoichiometric ratio.

The product was measured by high-resolution SR-PXD (BM01B) and PND (PUS, JEEP11). A structure predicted from DFT calculations was taken as the starting point for combined Rietveld refinement. The predicted orthorhombic  $\text{Ca}(\text{BF}_4)_2$ -type structure was basically confirmed ( $a = 13.4491(27)$  Å  $b = 9.5334(19)$  Å  $c = 9.0203(20)$  Å, space group  $Pbca$ ). The Ca atom is coordinated by 8 D from 8 different  $\text{AlD}_4$ -ions in a square antiprismatic way. The overall structure is layered, with empty plans parallel to the  $bc$ -plane (Figure 10).

A manuscript is in the final state of preparation and will be submitted to Inorganic Chemistry.

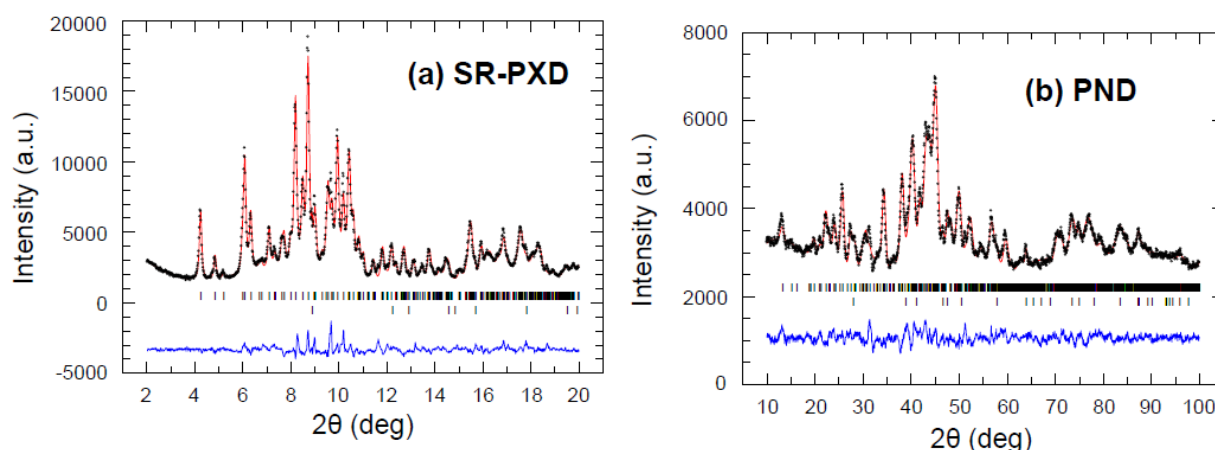


**Figure 9** Rietveld fits of  $\text{Ca}(\text{AlD}_4)_2$  to a) SR-PXD data and b) PND data. Upper and lower tick marks show Bragg peaks from  $\text{Ca}(\text{AlD}_4)_2$  solid solution and  $\text{AlD}_3$ , respectively.

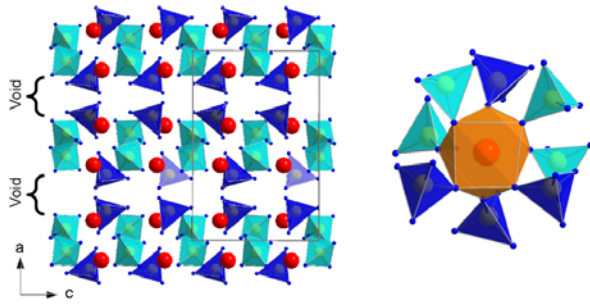


**Figure 10** The crystal structure of  $\text{Ca}(\text{AID}_4)_2$  (left). The coordination of Ca is outlined (right)

### **$\text{Li}_2\text{ND}$**

$\text{Li}_2\text{NH}$  (lithium imide) is an intermediate product in several reactions considered for hydrogen storage. Its crystal structure is not unambiguously determined. The most thorough investigation was performed by Balogh et al by SR-PXD and PND on a deuterated sample,  $\text{Li}_2\text{ND}$ . They found 3 structure models, one disordered cubic ( $a \sim 10 \text{ \AA}$ ) and two ordered orthorhombic (pseudo-cubic), which described the experimental data equally well. Above ca.  $90^\circ\text{C}$ , the phase took a (more) disordered face-centered cubic structure ( $a \sim 5 \text{ \AA}$ ).

A double isotope substituted lithium imide sample,  $^7\text{Li}_2\text{ND}$ , was prepared to clarify the room-temperature structure.  $^7\text{Li}$  was used due to its far smaller absorption cross section for neutrons than natural Li. PND (PUS, JEEPII) show several weak peaks that are inconsistent with cubic symmetry.

SR-PXD measurements at BM01B were collected at room temperature and  $100^\circ\text{C}$ . The  $100^\circ\text{C}$  pattern could be indexed according a small cubic unit cell with unit cell axes of half of that suggested by Balogh et al ( $a \sim 5 \text{ \AA}$ ). The RT pattern is noticeably different in two aspects: 1) there are additional peaks and 2) the cubic peaks are split into multiplets. The first point indicates an enlargement of the unit cell and the second point indicates lattice deformation. None of the unit cells suggested previously are consistent with the present data.

Supplementary PND data from PUS show the same additional peaks, but with higher relative intensity as the SR-PXD data. Structure determination is in progress.



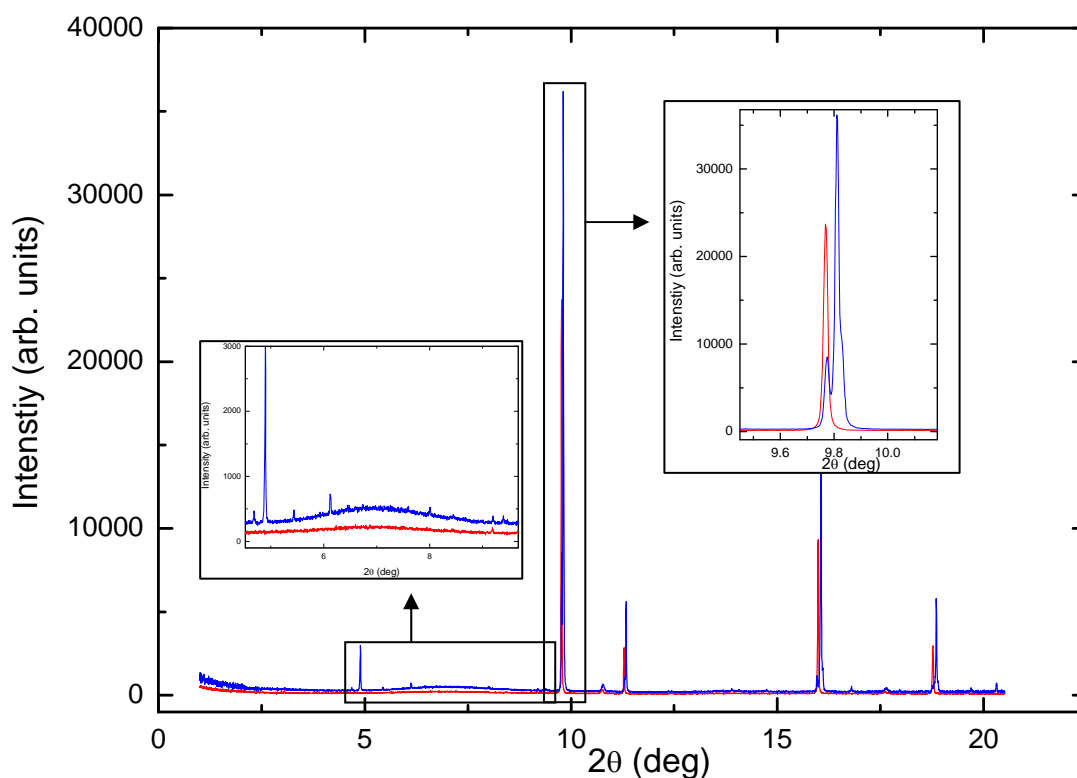


**Figure 11 SR-PXD data for 7Li<sub>2</sub>ND at RT (blue) and 100oC (red). Insets show ordering reflections (left) and peak splitting (right) at RT.**

### **LiBH<sub>4</sub> in carbon aerogel**

Preparation of LiBH<sub>4</sub> as nanoscopic particles is a possible route to lower the hydrogen desorption temperature.

LiBH<sub>4</sub> embedded in a carbon aerogel with a nominal pore size of 25 Å was measured at BM01B. The Bragg peaks were severely broadened compared to bulk LiBH<sub>4</sub> (Figure 12). The particle size was estimated to 20.3(7) nm using Rietveld refinement the Scherrer formula. It was assume to be no peak broadening from strain.

The result is not yet published but is expected to be included in a later publications.

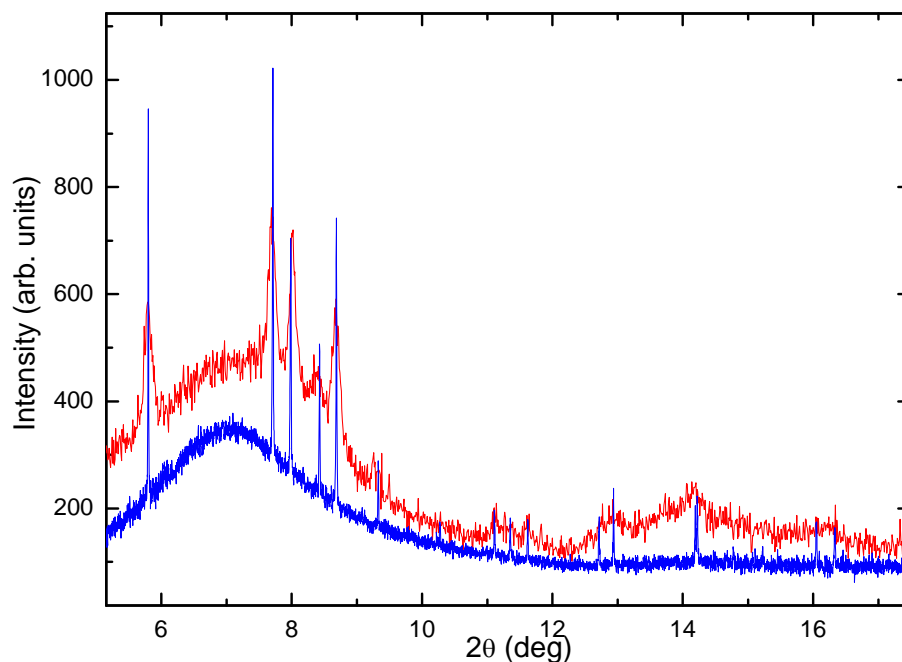


**Figure 12 Bulk LiBH<sub>4</sub> (blue) and LiBH<sub>4</sub> embedded in a carbon aerogel (red).**

### **Transition metal (TM)-aluminium phases in TM-enhanced NaAlH<sub>4</sub>**

An extensive investigation of performance and phase formation in TM-enhanced NaAlH<sub>4</sub> has been undertaken. The work is heavily based on SNBL beam time outside this long-term project, but since a significant amount of measurements were done with beam time from this project, it should be mentioned here.

A major result of the investigation concerns the whereabouts of the TM (typically Ti) after it is added to NaAlH<sub>4</sub>, since no crystalline TM-containing phases are observed by diffraction. Careful examination of high-resolution SR-PXD data of NaAlH<sub>4</sub> treated with different TM-salts, show amorphous halos which can be assigned to amorphous TM-Al phases (Figure 13). The observations have been backed up by high-resolution TEM.

A small part of the results are published in *Acta Materialia* [8] but a series of five papers presenting the bulk of the results, are under preparation and will be submitted to *Phys. Rev. B*.

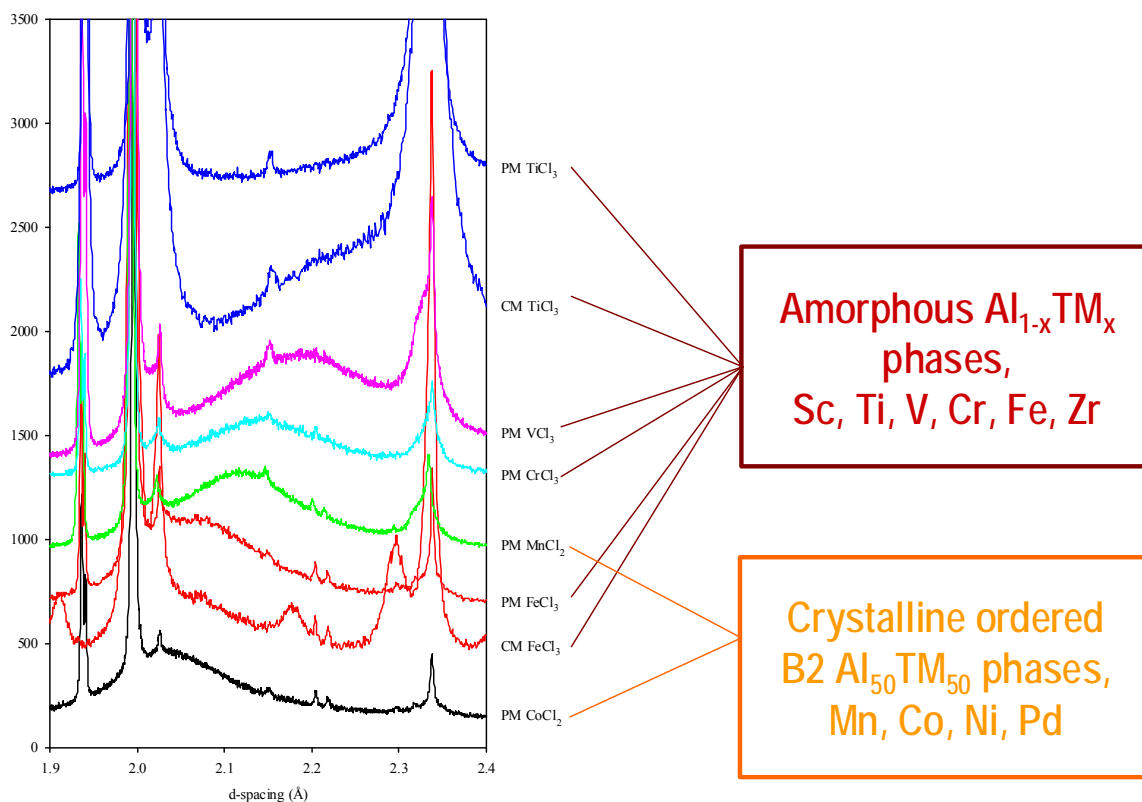


**Figure 13 High-resolution SR-PXD data of NaAlH<sub>4</sub> with different TM-chloride additives. Note the diffuse halos from amorphous TM-Al-phases.**

- [1] Grove, H.; Brinks, H.W.; Heyn, R.H.; Wu, F.J.; Opalka, S.M.; Tang, X.; Laube, B.L.; Hauback, B.C.: The structure of LiMg(AlD<sub>4</sub>)(3). *J. Alloys Comp.* **455** (2008) 249-254
- [2] Grove, H.; Brinks, H.W.; Lovvik, O.M.; Heyn, R.H.; Hauback, B.C.: The crystal structure of LiMgAlD<sub>6</sub> from combined neutron and synchrotron X-ray powder diffraction. *J. Alloys Comp.* **460** (2008) 64-68
- [3] Brinks, H.W.; Fossdal, A.; Hauback, B.C.: Adjustment of the stability of complex hydrides by anion substitution. *Journal of Physical Chemistry C* **112** (2008) 5658-5661
- [4] Riktor, M.D.; Sorby, M.H.; Chlopek, K.; Fichtner, M.; Buchter, F.; Zuettel, A.; Hauback, B.C.: In situ synchrotron diffraction studies of phase transitions and thermal decomposition of Mg(BH<sub>4</sub>)(2) and Ca(BH<sub>4</sub>)(2). *Journal of Materials Chemistry* **17** (2007) 4939-4942
- [5] Riktor, M.D.; Sørby, M.H.; Chlopek, K.; Fichtner, M.; Hauback, B.C.: The identification of an hitherto unknown intermediate phase CaB<sub>2</sub>H<sub>x</sub> from decomposition of Ca(BH<sub>4</sub>)<sub>2</sub>. *Journal of Materials Chemistry* DOI: **10.1039/B818127F** (2009)
- [6] Hagemann, H.; Longhini, M.; Kaminski, J.W.; Wesolowski, T.A.; Cerny, R.; Penin, N.; Sorby, M.H.; Hauback, B.C.; Severa, G.; Jensen, C.M.: LiSc(BH<sub>4</sub>)(4): A novel salt of Li<sup>+</sup> and discrete Sc(BH<sub>4</sub>)(4)(-) complex anions. *Journal of Physical Chemistry A* **112** (2008) 7551-7555
- [7] Deledda, S.; Hauback, B.C.: Formation mechanism and structural characterization of the mixed transition-metal complex hydride Mg<sub>2</sub>(FeH<sub>6</sub>)<sub>0.5</sub>(CoH<sub>5</sub>)<sub>0.5</sub> obtained by reactive milling. *Nanotechnology* **accepted** (2009)
- [8] Pitt, M.P.; Vullum, P.E.; Sorby, M.H.; Sulic, M.P.; Jensen, C.M.; Walmsley, J.C.; Holmestad, R.; Hauback, B.C.: Structural properties of the nanoscopic Al<sub>85</sub>Ti<sub>15</sub> solid solution observed in the hydrogen-cycled NaAlH<sub>4</sub>+0.1TiCl<sub>3</sub> system. *Acta Materialia* **56** (2008) 4691-4701